CHAPTER V

Au/ZnO AND Au/ZnO-Fe_2O_3 PREPARED BY DEPOSITION-PRECIPITATION AND THEIR ACTIVITY IN THE PREFERENTIAL OXIDATION OF CO*

5.1 Abstract

Preferential CO oxidation in a H_2-rich stream over ZnO and ZnO-Fe_2O_3 supported nano-size Au catalysts prepared by the deposition–precipitation method has been investigated. The reactant gas mixture contained 1% CO, 1% O_2, 40% H_2, 0–10% CO_2, and 0–10% H_2O, with the balance being He, at a total flow rate of 50 ml/min. The result showed that the Au/ZnO catalyst calcined at 500°C displayed superior activity, giving complete CO conversion with the highest selectivity (~75%) at 50°C, whereas the Au/ZnO-Fe_2O_3 showed a marked improvement in activity under CO_2 and H_2O surroundings. In a two-stage reactor, it provided a comparable CO conversion and a better selectivity, about 10%, as compared to a single-stage reactor. The prepared catalysts were characterized by XRF, XRD, TEM, DR/UV-vis, and TPR.

Keywords: Preferential CO oxidation; Hydrogen purification; Au catalyst; ZnO; Fe_2O_3.

---

* Energy & Fuels, 23 (2009) 5084–5091.

5.2 Introduction

Many advantages of preferential CO oxidation (PROX) have been reported, not only in keeping the operating cost low, but also in decreasing the CO content to an acceptable level (<10 ppm) without the excess hydrogen consumption that occurs during catalytic methanation before the H_2-rich fuel can be fed into proton exchange membrane fuel cells (PEMFCs). The catalyst for the PROX of CO must be effective in removing CO from a reformate gas, in which the main component is hydrogen, which is supplied to the fuel cell. PROX has been extensively studied using a variety of metal (Au, Pt, Ru, and Rh) catalysts.[1–5] The most important requirements for the PROX catalysts that have to be operated in the gas streams containing an excess amount of H_2 are as follows[6]: high CO oxidation rate at low temperatures, high CO conversion at a wide operating temperature range (50–200°C), high selectivity (or the catalyst must not oxidize a significant quantity of H_2), and good resistance to deactivation in the presence of H_2O and CO_2 in the reformate stream. Au-containing catalysts are reported to have high CO conversion and selectivity at low temperature. Over the last decade, it has been reported that the catalytic activity of a Au catalyst is strongly related to the preparation method, which brings about a great difference in Au particle size and interaction with the support. The deposition–precipitation method is the most promising method for preparing a Au catalyst, which is effective in depositing Au with high dispersion. Haruta et al.[7] indicated that the deposition–precipitation (DP) technique has many advantages over the co-precipitation (CP) in that all active Au remains on the support surface and none of the active Au is buried within it. The high catalytic activities of Au-supported catalysts depend not only on the dispersion and size of the gold particles but also on the appropriate catalyst support, which is very important to obtain superior performance. A significant role of the catalyst support was found on the conversion, selectivity, and stability of the catalyst. For example, a ZnO catalyst support showed high potential for use in the PROX reaction, as reported by Iwasa et al.[8]. They investigated the catalytic activities of various supported Pd catalysts and found that the catalytic activities significantly changed with the supports used. The Pd/ZnO catalyst prepared by the precipitation method exhibited the highest CO conversion. In the case of a Au-based catalyst, Au

supported on ZnO has been investigated for the PROX[9,10] and it was revealed that Au (1.5%wt)–Pt (1.0%wt) supported on ZnO displayed the best PROX activity, giving high CO conversion (97.5%), and high stability for 500 h of testing. Hence, it can be expected that the performance of a Au catalyst can be enhanced by using ZnO as a catalyst support. In addition, there are many reports about using FeO_x to promote the performance of Pt catalysts, e.g. Pt/Al_2O_3, Pt/CeO_2, and Pt/TiO_2 in many reactions including CO oxidation and preferential CO oxidation.[11–14] The role of reducible oxide supports have been described by the diffusion of oxygen from the lattice at the edge of the Au active sites for the CO oxidation reaction.[15,16] It was thus interesting to study the effect of a mixed metal oxide support by adding Fe_2O_3 to a ZnO support. Moreover, the addition of a number of reactors to the PROX process exhibits a higher CO conversion and selectivity, which was selected as another method to boost the PROX performance.[17–19]

Therefore, in the present work, we have attempted to compare the low-temperature preferential CO oxidation in the presence of H_2 over Au/ZnO and $Au/ZnO-Fe_2O_3$ prepared by deposition-precipitation. In obtaining the supported Au catalysts, the effects of calcination temperature and mixed oxide support on the catalytic activity were studied. The catalytic activity of the prepared catalysts was tested under a realistic reformate containing CO_2 and H_2O. The catalyst was tested at constant temperature to observe the durability with time-on-stream in a two-stage reactor to monitor the process performance.

5.3 Experimental

5.3.1 Catalyst Preparation

The ZnO support was synthesized by the precipitation method. An aqueous solution of 1 M Na_2CO_3 was added dropwise into a 0.1 M $Zn(NO_3)_3.6H_2O$ solution under vigorous stirring at 80°C.[20] The mixture was kept at pH 8 for 1 h. Excess ions, Cl^- and NO_3^-, were eliminated by washing with warm deionized water. The precipitate was dried at 110°C overnight and calcined in air at 400°C for 4 h. Nano-size Au deposition on ZnO, with a Au loading of 1% atom, was prepared by the

deposition–precipitation method, using 0.1 M Na_2CO_3 as a precipitating agent. An aqueous solution of $HAuCl_4.3H_2O$ was heated to 80°C, and ZnO was then added to this solution. Subsequently, the pH was adjusted to 8.0 by the addition of 0.1 M Na_2CO_3 under vigorous stirring. The temperature of the slurry was maintained at this temperature for 1 h. After the deposition of Au onto the support, the precipitate was filtered and washed carefully until the disappearance of NO_3^- and Cl^- ions. The Au/ZnO catalysts were dried at 110°C overnight and calcined in air at different temperatures (300, 400, and 500°C) for 4 h. The $ZnO-Fe_2O_3$ support at a 5:1 Zn:Fe molar ratio was prepared by co-precipitation using aqueous solutions of $Zn(NO_3)_2.3H_2O$ and $Fe(NO_3)_3.9H_2O$. The support was dried at 110°C overnight and then calcined at 400°C for 4 h. For Au supported on $ZnO-Fe_2O_3$, the catalysts were prepared by the same method, as described previously.

5.3.2 Characterization Techniques

The XRD measurements were performed on a Rigaku X-ray diffractometer system (RINT-2200) with a CuK_α X-ray source (λ=0.15405 nm) operating at 40 kV and 30 mA in order to obtain the diffraction patterns of the prepared catalysts and to determine the crystallite size of the Au on the surface (d_{XRD}), calculated by the Scherrer formula. The average Au sizes of the prepared catalysts were determined by TEM on a JEOL JEM 2010 operated at an accelerating voltage of 200 kV in bright field mode. The average Au size diameter (d_{TEM}) was calculated from the following formula: $d_{TEM} = \Sigma(n_i d_i)/n_i$, where n_i is the number of Au particles of diameter d_i. DR/UV-vis spectroscopy experiments were recorded on a Shimadzu UV spectrophotometer 2550. The measurements were performed on air-exposed samples at ambient temperature between 200 and 800 nm. The absorption intensity was expressed using the Kubelka-Munk function: $F(R\infty) = (1-R\infty)^2/2R\infty$, where $R\infty$ is the diffuse reflectance from a semi-infinite layer. Temperature-programmed reduction (H_2-TPR) analysis is used to check the presence of different states of oxidation of the contained metals. The weight of the tested samples was 60 mg. Prior to the analysis, the samples were pretreated in a flow of N_2 (20 $mlmin^{-1}$) at 100°C for 30 min. TPR tests were carried out in a micro-reactor with a TCD detector under a

flow of 5% H_2/N_2 gas mixture (30 $mlmin^{-1}$) and a heating rate of 10°$Cmin^{-1}$ from room temperature to 600°C. An Oxford ED 2000 EDXRF spectrometer and an AAS, VARIAN SpeactrAA model 300/400, were used for the determination of the Au content in the prepared catalysts.

5.3.3 Catalytic Activity

In the single-stage reactor process, the PROX was carried out in a fixed-bed U-tube microreactor by packing it with 100 mg of the catalyst (80–120 mesh). The activity was investigated at various temperatures in the range of 30 to 130°C under atmospheric pressure. In the double-stage reactor process, the reactors were serially connected. The amount of catalyst in each stage was packed equally with 50 mg. The catalytic activity and process performance were investigated at 50°C. (Each stage had its own O_2 supply and a temperature controller to control the reaction temperature.) The amount of O_2 entering each stage was controlled at a split ratio of 50:50. The outlet products from the first reactor were sent directly to the second reactor. No catalyst pretreatment process was used before any of the reaction tests. The composition of the inlet gases was 1% CO, 1% O_2, and 40% H_2, balanced in He, with a total flow rate of 50 $mlmin^{-1}$. The outlet gas from the reactor was analyzed by auto-sampling in an on-line gas chromatograph equipped with a packed carbosphere (80/100 mesh) column (10 ft x 1/8 inch) and a thermal conductivity detector (TCD). The CO and O_2 conversion were calculated based on the consumption of reactant gases. The selectivity was defined as the ratio of O_2 consumption for the desired CO oxidation reaction to the total O_2 consumption. The methanation, water gas shift (WGS), and reverse water gas shift (RWGS) reactions were found to be negligible over the tested temperature range.

5.4 Results and Discussion

5.4.1 Catalyst Characterization

The XRD patterns of the ZnO, Au/ZnO, and Au/ZnO-Fe_2O_3 catalysts are illustrated in Figure 5.1. Typical XRD patterns of ZnO zincite (JCPDS 50664) were

observed over the synthesized ZnO and Au/ZnO calcined at three different temperatures (300, 400, and 500°C) at 2θ of 31.78°, 34.48°, 36.28°, 47.56°, 56.62°, 62.94°, 66.54°, 67.98°, 69.12°, and 77.10°, which are the characteristic of (100), (002), (101), (102), (110), (103), (200), (112), (201), and (202) diffraction peaks of ZnO, respectively. For the catalysts calcined at 300 and 400°C, it was found that the Au particles were highly dispersed on the surface of the support or that they are too small to be detected by this technique, and/or the metallic Au peaks or gold oxides Au_2O_3 were overlapped by zincite.[21] All peaks of the samples calcined at different temperatures did not change significantly; however, the Au/ZnO calcined at 500°C showed the diffraction peak of Au(111) at 2θ=38.20°. In the sample containing Fe_2O_3, the diffraction peaks correspond to $ZnFe_2O_4$ (220), $ZnFe_2O_4$ (311), and $ZnFe_2O_4$ (400), revealing that the ZnO phase is present in the $ZnFe_2O_4$ composite particles or that some of the Fe_2O_3 has been incorporated in the ZnO lattice due to the fact that the lattice parameters were $a_{\alpha\text{-}Fe2O3}$ = 1.375 nm, $b_{\alpha\text{-}Fe2O3}$ = 0.872 nm[22], a_{ZnO} = 3.244 nm, and c_{ZnO} = 5.297 nm.[23]

After 12 h of the experiment, it was found that the intensities of the XRD patterns of the spent catalysts were slightly lower than that of the fresh catalysts (Figure 5.1 (d–g)) and no phase transformation was observed, implying that the catalytic performance of the prepared catalyst can be kept stable during the 12 h reaction.

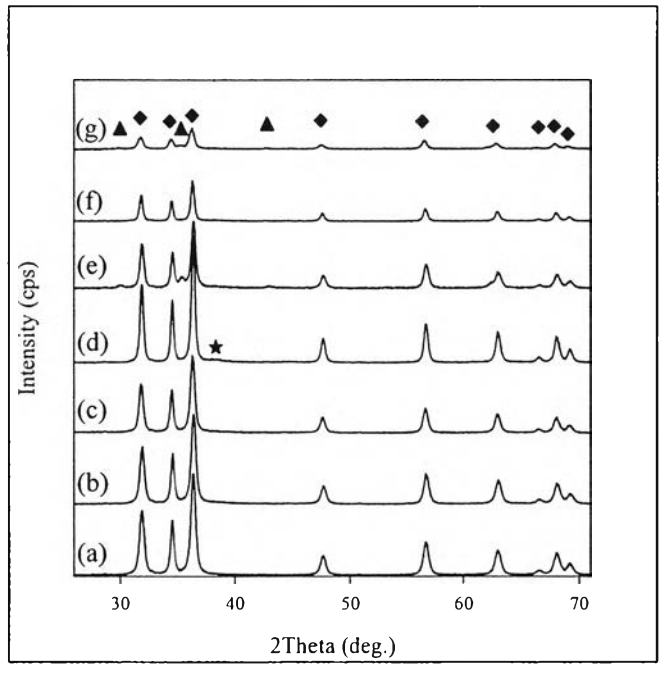

Figure 5.1 XRD patterns of Au supported on ZnO at different calcination temperatures and spent catalysts: (★) Au 111; (◆) ZnO; (▲) $ZnFe_2O_4$; (a) pure ZnO; (b) Au/ZnO calcined at 300°C; (c) Au/ZnO calcined at 400°C; (d) Au/ZnO calcined at 500°C; (e) Au/ZnO-Fe_2O_3 calcined at 500°C; (f) spent Au/ZnO calcined at 500°C; and, (g) spent Au/ZnO-Fe_2O_3 calcined at 500°C.

It has been reported that the PROX activity was strongly correlated with a suitable Au particle size. The catalysts with gold particles smaller than 5 nm can be able to catalyze the CO oxidation at temperatures as low as 0°C[7]; however, it is not a practical operating temperature for PEMFC applications. The TEM technique was subsequently employed to confirm the Au particle size of the prepared catalysts. Small Au particles, ultra finely dispersed with almost the same size, are clearly observed on the ZnO and ZnO-Fe_2O_3 supports in the TEM micrographs, as shown in Figure 5.2 (a and b). The Au particles are seen as dark contrasts on the surface of the ZnO and ZnO-Fe_2O_3 particles. The presence of Au on the ZnO support was confirmed by energy dispersive spectroscopy (EDS). For the Au/ZnO calcined at 500°C, metallic Au peaks are clearly present because the average particle size of this catalyst, by TEM, is particularly larger than 5 nm, as shown in the percentage of distribution. The higher calcination temperature is attributed to the aggregation of Au

particles during the preparation step. The mean particle size of the Au over Au/ZnO and Au/ZnO-Fe_2O_3 catalysts were 4.9 ± 1.0 and 3.2 ± 1.1 nm, respectively. These observations indicate a strong influence of support catalyst on the Au particle size of the metal oxide-supported Au catalysts, which were prepared by the same method. It suggests that the introduction of Fe_2O_3 could lead to a decrease of the average Au particle size. Kang and Wan also found that stabilization of Au particle size in the Au/zeolite Y was observed by the addition of Fe_2O_3.[24] The Au particles on the ZnO-Fe_2O_3 were widely distributed from 1 to 7 nm, as shown in Figure 5.2(b), while the Au particle size distribution of the Au/ZnO had a narrower range (Figure 5.2(a)).

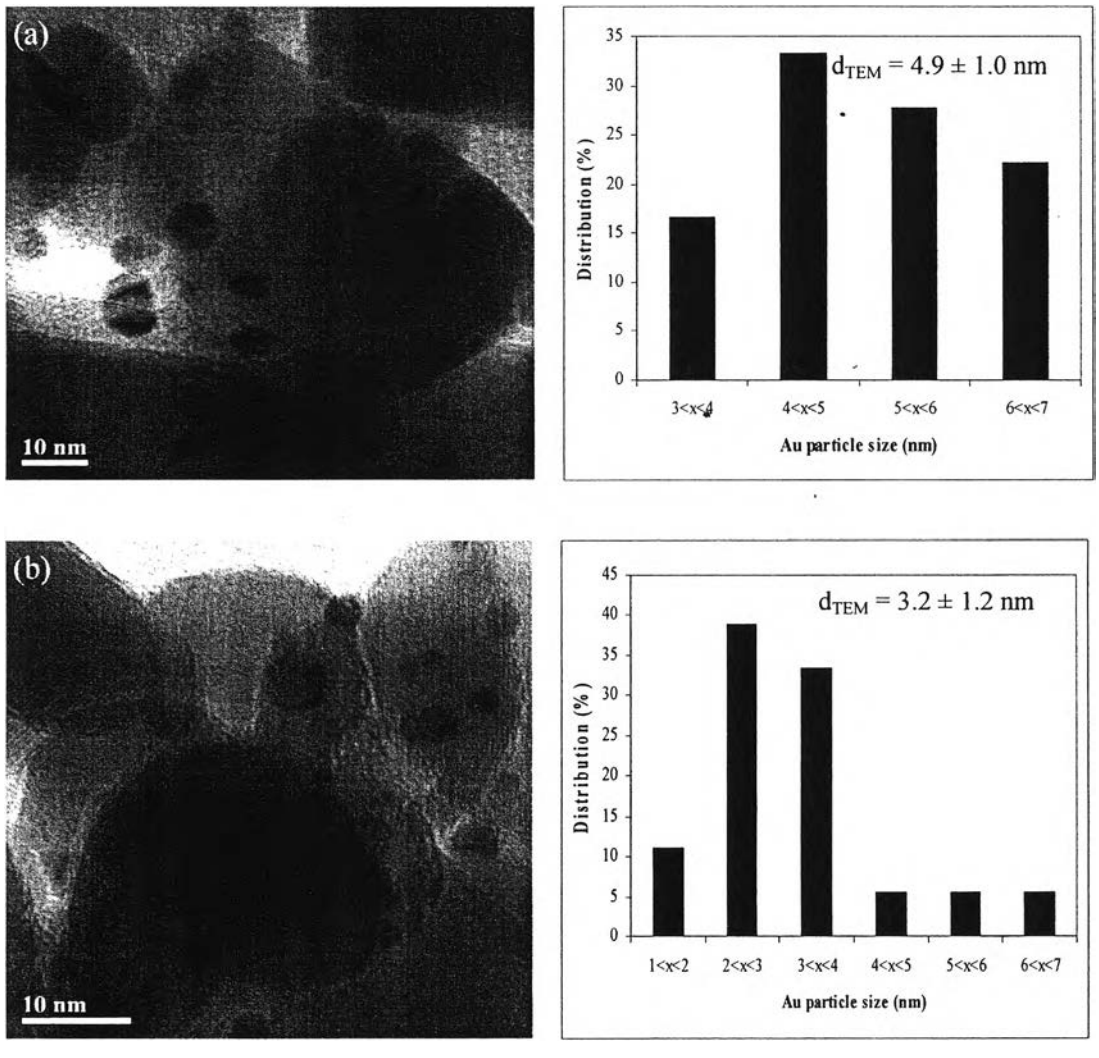

Figure 5.2 TEM images and Au particle size distribution of the prepared catalysts, which were calcined at 500°C: (a) Au/ZnO and (b) Au/ZnO-Fe_2O_3.

In order to further confirm the attribution of the XRD and TEM results, the DR/UV-vis absorption spectra of both catalysts were used to analyze the gold species in the samples, as shown in Figure 5.3A. However, the ZnO shows absorption bands in the range of 200–350 nm[25]; therefore, the presence of gold clusters at 280–380 nm and Au^{3+} at <250 nm cannot be observed. In the case of the Au/ZnO, an intense peak is clearly observed at ~550 nm, which is due to the surface plasma absorptions of gold nanoparticles, and the intensity of the UV emission of Au/ZnO is higher than that of the Au/ZnO-Fe_2O_3. These results are in accordance with the XRD and TEM results, suggesting that the Au particles of Au/ZnO are larger than those of the Au/ZnO-Fe_2O_3. The TPR profiles of the samples are shown in Figure 5.3B(a–d). The ZnO sample and the Au/ZnO sample calcined at 500°C did not show strong reduction peaks; however, both supported Au catalysts show reduction peaks within the interval of 150–200°C (Figure 5.3B), which are assigned to the Au^{3+} reduction.[26] The Au/ZnO calcined at 500°C has a very low intensity reduction peak (Au^{3+}) and a lower reduction temperature than the Au/ZnO-Fe_2O_3 calcined at 500°C. The TPR profile of the ZnO-Fe_2O_3 reveals the overlap peak in the temperature range of 250–550°C, corresponding to the reduction step of Fe_2O_3 to Fe_3O_4 at the lower temperature peak and the transition of Fe_3O_4 to FeO to Fe at the higher temperature peak.[27] When a small amount of Au was loaded onto the ZnO-Fe_2O_3 support, it was observed that the first peak (~400°C) was significantly reduced. Based on the TPR results, it can be concluded that the reducible mixed metal oxide support was particularly changed when applying the high calcination temperature (500°C) to prepare the catalyst. In addition, the reduction peaks at high temperatures (>600°C) represent the reduction of the bulk phase of the samples. The actual Au content in the catalysts was measured by the XRF and AAS (not shown) and the result demonstrated that the Au loadings in the prepared catalysts were very close to the calculated value (about 0.7–0.9 %atom).

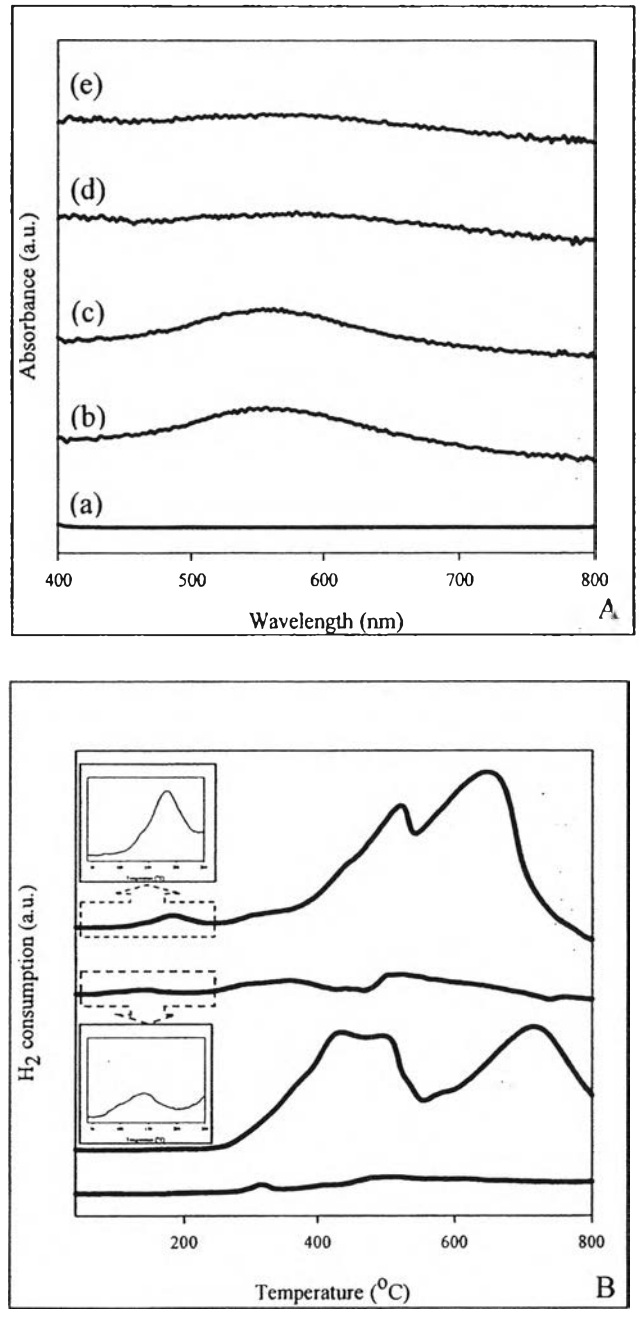

Figure 5.3 (A) DR/UV-vis spectra of the prepared catalysts and the spent catalysts: (a) ZnO, (b) Au/ZnO calcined at 500°C, (c) spent Au/ZnO, (d) Au/ZnO-Fe_2O_3 calcined at 500°C, and (e) spent Au/ZnO-Fe_2O_3.

(B) TPR profiles of the prepared catalysts and supports: (a) ZnO, (b) ZnO-Fe_2O_3, (c) Au/ZnO calcined at 500°C, and (d) Au/ZnO-Fe_2O_3 calcined at 500°C.

5.4.2 Effect of Calcination Temperature

Figure 5.4 (a–c) shows the results of the PROX activity catalyzed by the Au/ZnO catalysts at various calcination temperatures as a function of temperature. The calcination temperature was varied from 300 to 500°C and the percent loading of Au was kept at 1% by atom. The results revealed that the 1%Au/ZnO calcined at 500°C exhibited the highest activity, which provided almost 100% CO conversion, and 75% selectivity at 50°C. The O_2 conversion profiles of all the catalysts followed a similar trend, but there was a difference in the temperature reaching 100% (Figure 5.4c). The catalysts calcined at 300 and 400°C exhibited a higher CO conversion at 30°C, whereas the catalyst calcined at 500°C achieved 100% CO conversion at a high temperature range (50–130°C), although the catalysts calcined at low temperatures generally contain small Au crystallites, resulting in more active catalysts than those calcined at higher temperatures, which is the suitable operating temperature of the PROX unit for PEMFC applications at a temperature range of 50–70°C. The catalytic activity does not only depend on the Au crystallite size but also relates to the metal–support interaction and the phase of the catalyst support. Additional information will be sought to further clarify and understand the correlations.

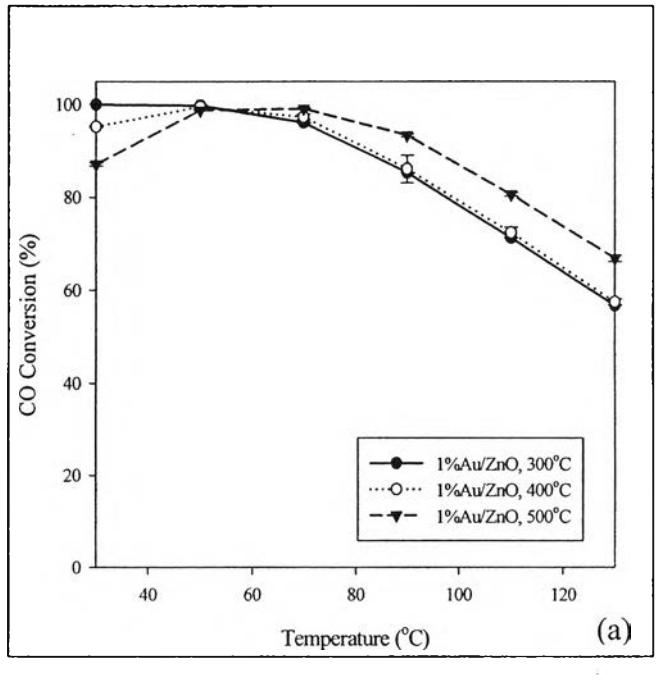

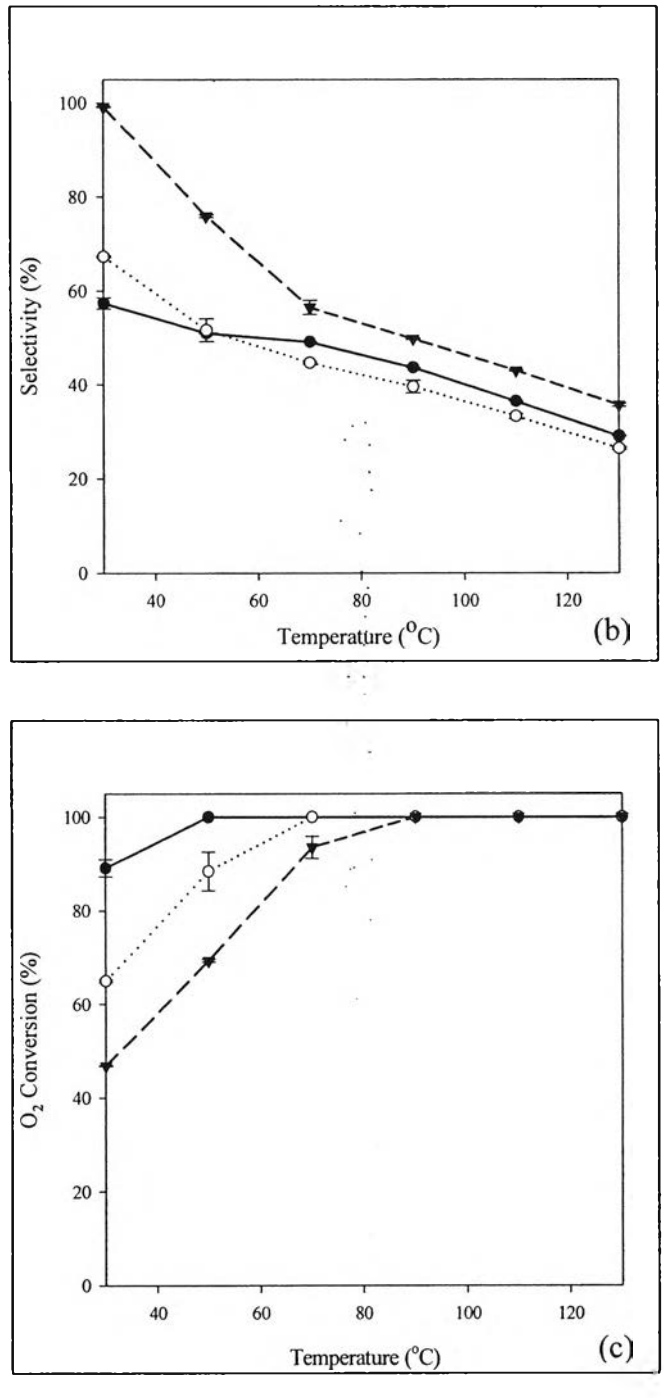

Figure 5.4 Effect of calcination temperature on 1%Au/ZnO catalysts: (●) 300°C, (○) 400°C, and (▼) 500°C. (a) CO conversion, (b) selectivity, and (c) O_2 conversion.

5.4.3 Effect of Mixed–Oxide Support on the Performance of Au Catalyst

Small Au particle size is not the only necessary criterion for high activity; the strong interaction of the Au particles with the support is also very important. In this work, the 1%Au/ZnO-Fe_2O_3 calcined at 500°C at a 5:1 molar ratio of ZnO/Fe_2O_3 was prepared, and its activity was compared with Au/ZnO calcined at 500°C, as shown in Figure 5.5. It was found that the CO conversions of both Au/ZnO and Au/ZnO-Fe_2O_3 were maintained above 98% at 50–70°C. On the other hand, the selectivity of the Au/ZnO catalyst was slightly higher than that of the Au/ZnO-Fe_2O_3 catalyst in the same temperature range. The observed effect of the selectivity of the Au/ZnO can be explained by the relatively weak interaction of the Au with the support, observed by TPR (Figure 5.3B). The Au/ZnO-Fe_2O_3 catalyst, however, insignificantly changed the O_2 consumption rate of the catalyst. This can be described by the role of Fe_2O_3, which provides alternative oxygen for both the CO oxidation and the H_2 oxidation, resulting in a decrease of the selectivity. These results are in good agreement with Korotkikh and Farrauto[28], who suggested that the metal oxide promoter provides sufficient dissociated O_2 to enhance the oxidation rate. The catalytic performance of the Au/Fe_2O_3 in this reaction is strongly related to the support phase, being sensitive to the microcrystalline structure and the oxidation state of the Fe_2O_3.[29] The results can also be confirmed by the TPR profiles, as illustrated in Figure 3B. The H_2 consumption peak area of the ZnO-Fe_2O_3 support is much larger than the pure ZnO support, suggesting that the ZnO-Fe_2O_3 could provide more oxygen than ZnO; consequently, the selectivity of the Au/ZnO-Fe_2O_3 was reduced. Additionally, ZnO and ZnO-Fe_2O_3 have no noticeable catalytic activities for the PROX in the tested temperature range.

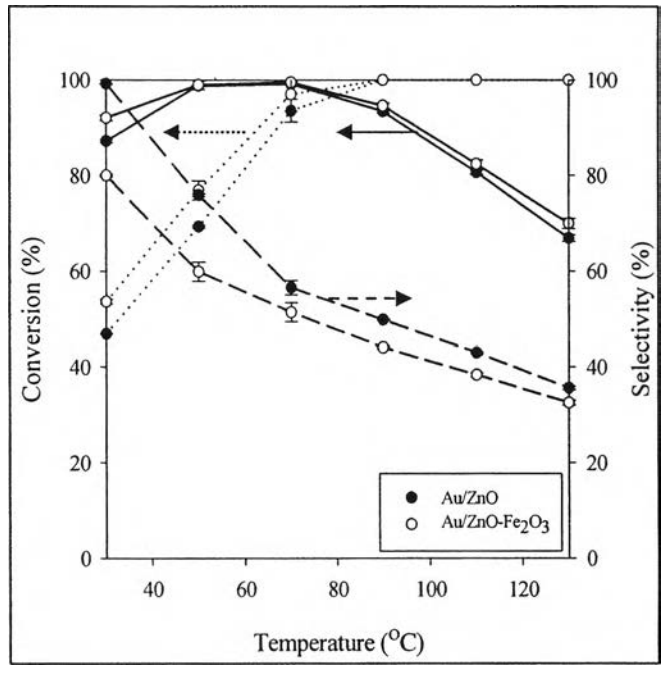

Figure 5.5 Effect of mixed oxide support: (●) Au/ZnO calcined at 500°C and (○) Au/ZnO-Fe_2O_3 calcined at 500°C. CO conversion (—), selectivity (– –), and O_2 conversion (·····).

5.4.4 Effect of H_2O Vapor on the Catalytic Performance

The effect of the H_2O vapor present in the feedstream on the catalytic performance of the Au/ZnO and Au/ZnO-Fe_2O_3 catalysts was investigated. The influence of H_2O on the CO oxidation reaction over supported Au catalysts has been investigated by several researchers.[30–32] The catalytic activities of the catalysts were tested with a reactant gas composition of 10%H_2O, 1%CO, 1%O_2, and 40%H_2, balanced in He. As shown in Figure 5.6, the presence of H_2O vapor had a significantly negative effect on the CO conversion of the Au/ZnO catalysts, but it had no significant effect on that of the Au/ZnO-Fe_2O_3 over the entire temperature range investigated. We proposed that the inhibition effect of H_2O is due to adsorption of the H_2O molecule on the active site and/or on the catalyst support, or due to condensation within the pore. The difference in catalytic activities between the Au/ZnO and the Au/ZnO-Fe_2O_3 can be explained by the role of Fe_2O_3, which has more stored oxygen. The Fe_2O_3 can provide more active oxygen from lattice oxygen

than the pure ZnO, even when H_2O molecules are adsorbed on the catalyst support. Therefore, the negative effect of H_2O was more pronounced with the Au supported on ZnO, but became negligible with the Au supported on ZnO-Fe_2O_3. The extent of the H_2O effect depends strongly on the reaction temperature. At the lower temperature, the CO conversions of both catalysts were significantly reduced. At higher temperature (50–130°C), the addition of H_2O had almost no, or even a slightly positive, effect on the CO conversion. When water was added to the feed, it increased the selectivity of the Au/ZnO-Fe_2O_3 from 60 to 70% at 50°C since it tended to suppress hydrogen oxidation, especially at the low temperature range. Under similar reaction conditions, the Au/ZnO-Fe_2O_3 is able to be operated in the presence of H_2O vapor in the feedstream. Based on these results, the mixed–oxide support (ZnO-Fe_2O_3) was found to be able to tolerate the high amounts of H_2O contained in the feedstream with a wide range of reaction temperature (50–130°C). Positive effects were revealed by several research groups for various types of supports. In the work of Schubert et al.[31], for example, they concluded that the main reason for the enhanced selectivity is a significantly diminished H_2 oxidation rate in the presence of H_2O. Furthermore, the CO oxidation can be enhanced by the formation of hydroxyl groups on the catalyst support where the adsorbed H_2O is a better oxidant than oxygen.[33] The positive H_2O effect on the ZnO catalyst support has also been reported by Manzoli et al.[34]. They studied the role of H_2O in the PROX reaction over Au/CeO_2 doped by ZnO by using FTIR spectrometry. They reported the beneficial role of H_2O with the appearance of a band at 1135 cm^{-1} in the FTIR spectra, collected during a CO+O_2 interaction in excess H_2 followed by the addition of H_2O. This band is related to the O_2 species and its presence can be taken as an indication of the ability of the catalyst to activate O_2. However, the water effect is due to neither a water gas shift nor reverse water gas shift reactions since they are negligible at these temperatures.

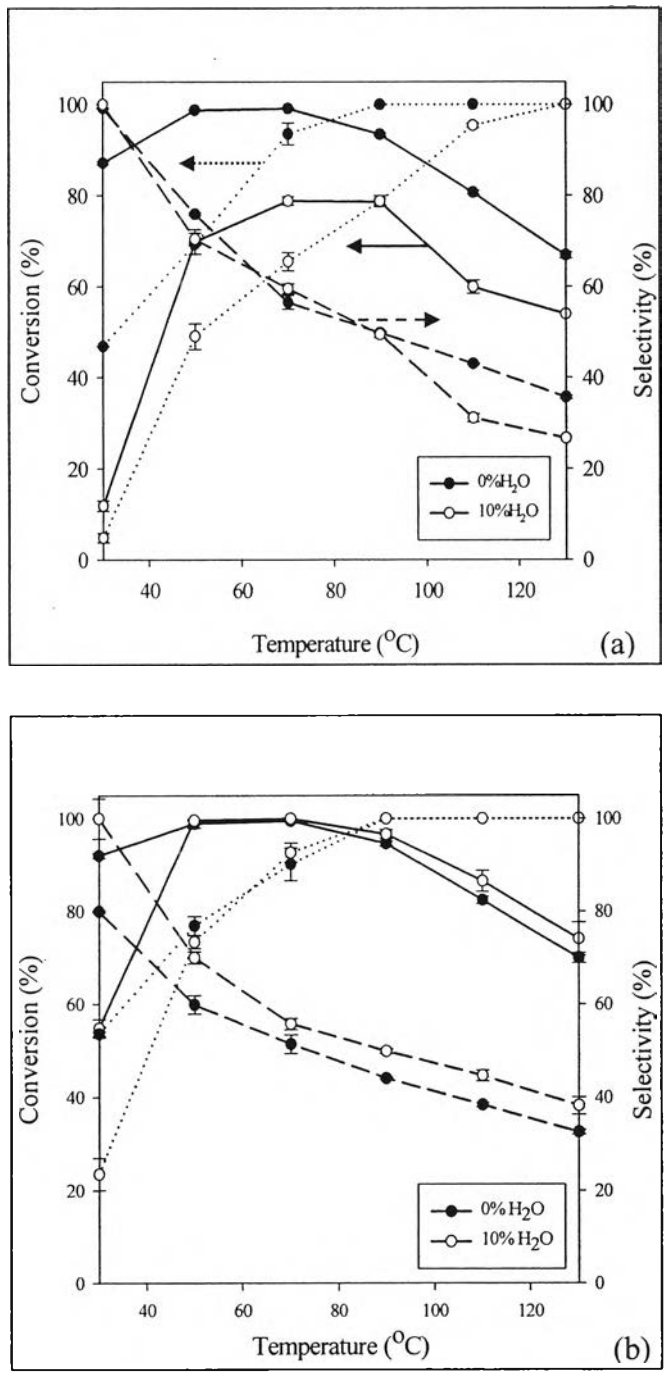

Figure 5.6 Effect of H_2O vapor on the catalytic performance: (a) Au/ZnO calcined at 500°C and (b) Au/ZnO-Fe_2O_3 calcined at 500°C (●) 0% H_2O and (○) 10% H_2O. CO conversion (—), selectivity (– –), and O_2 conversion (·····).

5.4.5 Effect of CO_2 on the Catalytic Performance

The outlet stream coming from the WGS reactor in the fuel processing usually contains 10–25% CO_2. As a result, the catalyst performance in the presence of a large volume of CO_2 in the simulated reformed gas has to be considered. The catalytic activities of the catalysts were tested with a reactant gas composition of 10%CO_2, 1%CO, 1%O_2, and 40%H_2, balanced in He. As shown in Figure 5.7, similar to the effect of the H_2O, the presence of CO_2 has a significantly negative effect on the catalytic activities of both the catalysts in the tested temperature range. The difference in the catalytic activities, with and without CO_2 in the feedstream, can be explained in that the interface between the support and the metal active sites contains mobile O_2, which is blocked by the CO_2 adsorbed on the same sites, resulting in the CO_2 suppressing the CO conversion and selectivity.[31] As a consequence of the H_2O effect, the Fe_2O_3 can provide more active oxygen even when the CO_2 molecule adsorbed on the surface of the catalyst support. The extent of the CO_2 effect depends strongly on the reaction temperature. At 30°C, the selectivity of both catalysts was significantly reduced, caused by the CO_2 more easily adsorbing on the surface at the lower temperature. Moreover, the CO_2 has a less negative effect on the Au/ZnO-Fe_2O_3 than on the Au/ZnO catalyst. At higher temperature (70–130°C), the addition of CO_2 had almost no, or even a slightly positive, effect on the catalytic activities in terms of both the CO conversion and the selectivity. The CO conversion was improved by 5% at 110°C and the selectivity was improved by 10% in the range of 70–90°C. From these results, it can be concluded that the Au supported on the mixed–metal oxide (ZnO-Fe_2O_3) catalyst shows a higher resistance toward CO_2 than the Au supported on ZnO alone in the presence of CO_2 in the feedstream.

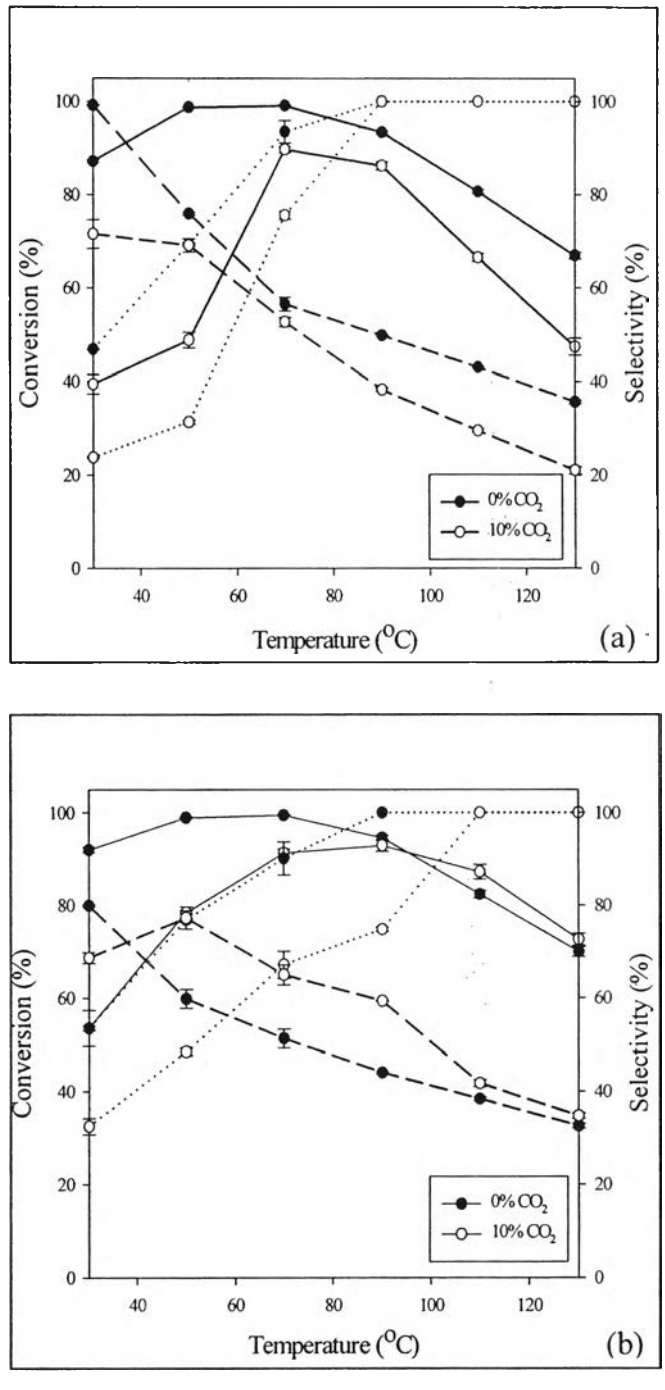

Figure 5.7 Effect of CO_2 on the catalytic performance: (a) Au/ZnO calcined at 500°C and (b) Au/ZnO-Fe_2O_3 calcined at 500°C. (●) 0% CO_2 and (○) 10% CO_2. CO conversion (—), selectivity (– –), and O_2 conversion (·····).

5.4.6 Effect of a Combination of CO_2 and H_2O on Catalytic Performance

In view of the important roles of CO_2 and H_2O in the PROX, an investigation of the influence of both CO_2 and H_2O over Au/ZnO and Au/ZnO-Fe_2O_3 was done in this present work, using a feed of 10%CO_2, 10%H_2O, 1%CO, 1%O_2, and 40%H_2, balanced in He. When comparing the activity of both catalysts from the CO conversion profiles in Figure 5.8, the presence of both CO_2 and H_2O in the feedstream diminished the CO conversions of both catalysts, especially in the low temperature range. The maximum CO conversion of both catalysts was shifted approximately 40°C higher and decreased to 90%. However, the selectivity of the Au/ZnO catalyst was insignificantly impacted by the presence of CO_2 and H_2O in feedstream. The presence of CO_2 and H_2O provoked a significant increase, however, in the selectivity of Au/ZnO-Fe_2O_3, achieving ~90% selectivity at 50°C. These results are in good agreement with Avgouropoulos et al.[35], who reported that the presence of CO_2 and H_2O in the feedstream over a Au/α-Fe_2O_3 catalyst reduced the CO conversion, but increased the selectivity. The O_2 consumption rate was slowed and reached 100% at a temperature of 110°C. The CO_2 had a stronger influence on the catalytic performance of both the Au/ZnO and the Au/ZnO-Fe_2O_3 catalysts than did the H_2O. Schubert et al.[31] concluded that the addition of CO_2 reduces the CO oxidation rate and selectivity, which was attributed to the co-adsorption of CO_2 on the Au particles or at the Au-metal oxide interface.

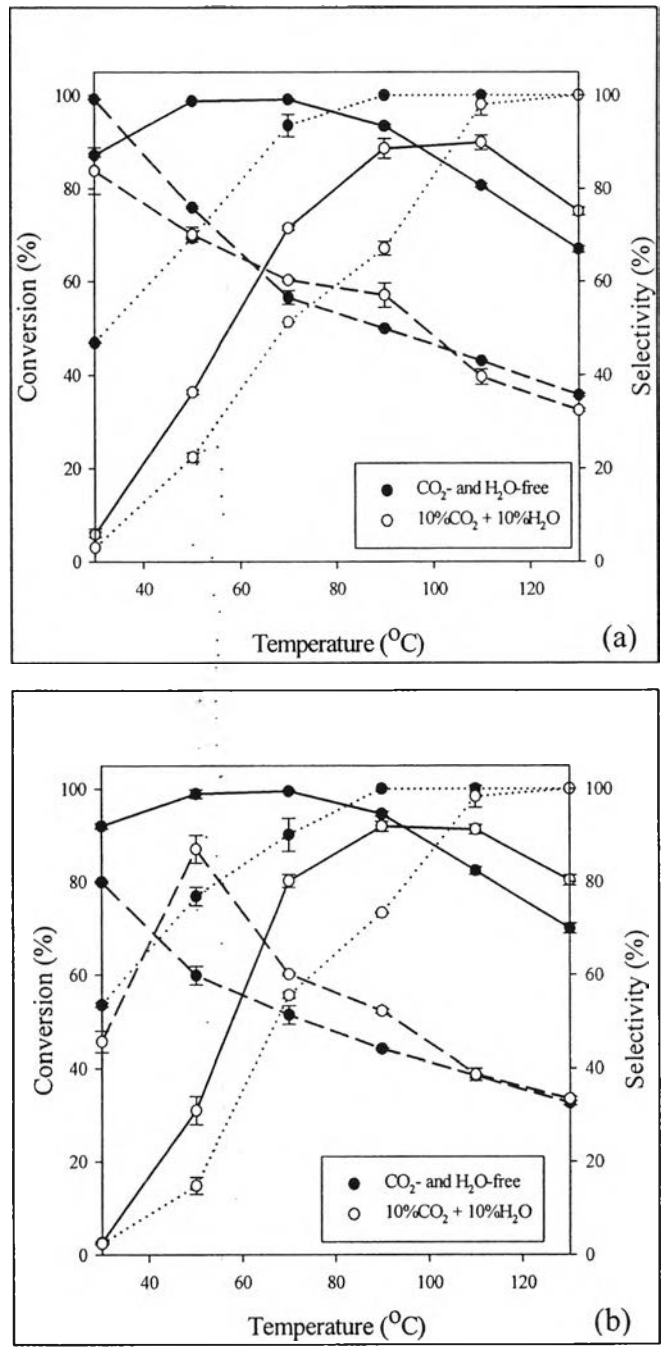

Figure 5.8 Effect of the combination of CO_2 and H_2O on the catalytic performance: (a) Au/ZnO calcined at 500°C and (b) Au/ZnO-Fe_2O_3 calcined at 500°C. (●) 0% CO_2 and (○) 10% CO_2. CO conversion (—), selectivity (– –), and O_2 conversion (·····).

5.4.7 Stability Testing

The catalytic activities of the 1% Au/ZnO and 1%Au/(5:1)ZnO-Fe_2O_3 were tested at constant temperature (50°C) for 12 h in order to observe the stability with time-on-stream. The PROX reaction was performed with a reactant gas composition of 1%CO, 1%O_2, and 40%H_2, balanced in He, which is the optimum temperature of these catalysts. In these operating conditions, low CO concentrations in the simulated reformate remained. There was no degradation observed over the catalysts for the PROX reaction during the 12 h testing time. These results can be noticeably confirmed by the XRD and UV results, as illustrated in Figures 5.1 and 5.3. There were no phases of the spent catalysts changed and metallic Au peaks did not appear in the XRD patterns.

5.4.8 Double-Stage System

The double-stage system was conducted under similar reaction conditions as the single-stage system except for the fractionation of the O_2 supplied to each reactor. The process performance was optimized at an O_2 split ratio of 50:50, which provided the maximum CO conversion and comparable selectivity, as reported in the previous work.[36] The catalytic reactors were serially arranged and each was packed with 50 mg of the Au/ZnO catalyst. The system performance was investigated at constant temperature of 50°C. Figure 5.9 shows that the double-stage system clearly gave a much higher selectivity (10%) at the same conditions as the single-stage system; and both systems provided a comparable CO conversion. From these results, we can confidently conclude that the double-stage system increased the process efficiency more than the single-stage system; it was superior to the single-stage system for the CO removal in a H_2-rich stream.

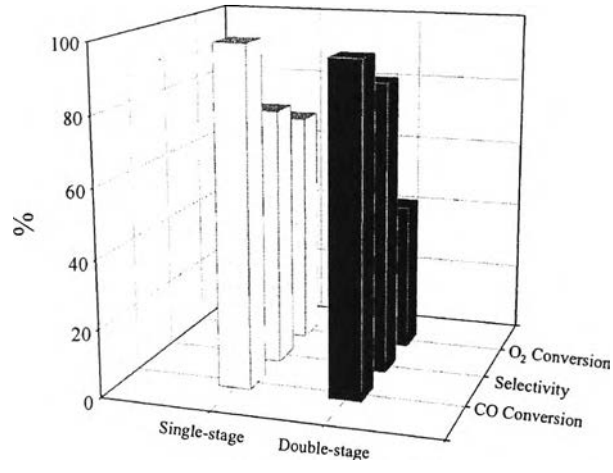

Figure 5.9 Comparison of the overall activity of the single- and double-stage process without CO_2 and H_2O in the feedstream over the Au/ZnO catalyst calcined at 50°C and 50:50, respectively.

5.5 Conclusions

Our results showed that both the Au/ZnO and the Au/ZnO-Fe_2O_3 catalysts exhibited high catalytic activities, where they achieved an almost complete conversion of CO to CO_2 at 50–70°C with 60–75% selectivity. Moreover, using the mixed-metal oxide support (ZnO-Fe_2O_3) resulted in improved resistance toward the presence of CO_2 and H_2O. Both catalysts were quite stable with time-on-stream. Additionally, the Au-oxide interface plays an important role in the PROX activity. The deposition of Au on supports with Na_2CO_3 is an effective method for creating smaller Au particles, resulting in an increase of the number of Au-oxide interfaces, which enhances the catalytic activity for this reaction.

5.6 Acknowledgements

This work was supported by the Thailand Research Fund (TRF) (MRG5080228), the Ratchadapisake Sompote Fund, and the Center for Petroleum, Petrochemicals and Advanced Materials, Chulalongkorn University. Special thanks go to Mr. Robert Wright for the English proof reading.

5.7 References

(1) Avgouropoulos, G.; Papavasiliou, J.; Tabakova, T.; Idakiev, V.; Ioannides, T. *Chem. Eng. J.* **2006**, 124, 41–45.

(2) Rosso, I.; Galletti, C.; Saracco, G.; Garrone, E.; Specchia, V. *Appl. Catal. B: Environ.* **2004**, 48, 195–203.

(3) Naknam, P.; Luengnaruemitchai, A.; Wongkasemjit, S.; Osuwan, S. *J. Power Sources* **2007**, 165, 353–358.

(4) Han, Y. F.; Kahlich, M. J.; Kinne M.; Behm, R. J. *Appl. Catal. B: Environ.* **2004**, 50, 209–218.

(5) Chen, X.; Zou, H.; Chen, S.; Dong, X.; Lin, W. *J. Nat. Gas Chem.* **2007**, 16, 409–414.

(6) Zhao, Z.; Yung M. M.; Ozkan, U.S. *Catal. Commun.* **2008**, 9, 1465–1471.

(7) Haruta, M.; Tsubota, S.; Kobayashi, T.; Kageyama, H.; Genet, M. J.; Delmon, B. *J. Catal.* **1993**, 144, 175–192.

(8) Iwasa, N.; Arai, S.; Arai, M. *Catal. Commun.* **2006**, 7, 839–842.

(9) Zhang, J.; Wang, Y.; Chen, B.; Li, C.; Wu, D.; Wang, X. *Energy Convers. Manage.* **2003**, 44, 1805–1815.

(10) Wang, Y. H.; Zhu, J. L.; Zhang, J. C.; Song, L. F.; Hu, J. Y.; Ong, S. L.; Ng, W. J. *J. Power Sources* **2006**, 155, 440–446.

(11) Shou, M.; Tanaka, K. I.; Yoshioka, K.; Moro-oka, Y.; Nagano, S. *Catal. Today* **2004**, 90, 255–261.

(12) Hodge, N. A.; Kiely, C. J.; Whyman, R.; Siddiqui, M. R. H.; Hutchings, G. J.; Pankhurst, Q. A.; Wagner, F. E.; Rajaram, R. R.; Golunski, S. E. *Catal. Today* **2002**, 72, 133–144.

(13) Qiao, B.; Deng, Y. *Chem Commun* **2003**, 17, 2192–2193.

(14) Luengnaruemitchai, A.; Osuwan, S.; Gulari, E. *Catal Commun* **2003**, 4, 215–221.

(15) Schubert, M. M.; Plzak, V.; Garche, J.; Behm, R. J. *Catal. Lett.* **2001**, 76, 143–150.

(16) Schubert, M. M.; Hackenberg, S.; Veen, A. C. V.; Muhler, M.; Plzak, V.; Behm, R. J. *J. Catal.* **2001**, 197, 113–122.

(17) Ahluwalia, R. K.; Zhang, Q.; Chmielewski, D. J.; Lauzze, K. C.; Inbody, M. A. *Catal. Today* **2005**, 99, 271–283.

(18) Srinivas, S.; Gulari, E. *Catal. Commun.* **2006**, 7, 819–826.

(19) Seo, Y. T.; Seo, D. J.; Jeong, J. H.; Yoon, W. L. *J. Power Sources* **2006**, 160, 505–509.

(20) Wang, G. Y.; Xiang, Z. W.; Lian, H. L.; Jiang, D. Z.; Wu, T. H. *Appl Catal A: Gen* **2003**, 239, 1–10.

(21) Yang, H. C.; Chang, F. W.; Roselin, L. S. *J. Mol. Catal. A: Chem* **2007**, 276, 184–190.

(22) Zhang, D. F.; Sun, L. D., Jia, C. J.; Yan, Z. G.; You, L. P.; Yan, C. H. *J. Am. Chem. Soc.* **2005**, 127, 13492–13493.

(23) Singh, P.; Kumar, A.; Kaushal, A.; Kaur, D.; Pandey, A.; Gonal, R. N. *Bull. Mater. Sci.* **2008**, 31, 573–577.

(24) Kang, Y. M.; Wan, B. Z. *Catal. Today* **1995**, 26, 59–69.

(25) Souza, K. R.; Lima, A. F. F.; Sousa, F. F.; Appel, L. G. *Appl. Catal. A: Gen.* **2008**, 340, 133–139.

(26) Sandoval, A.; Gómez-Cortés, A.; Zanella, R.; Díaz, G.; Saniger, J. M. *J. Mol. Catal. A: Chem.* **2007**, 278, 200–208.

(27) Ilieva, L. I.; Andreeva, D.; Andreev, A. A. *Thermochim. Acta* **1997**, 292, 169–174.

(28) Korotkikh, O.; Farrauto, R. *Catal. Today* **2000**, 62, 249–254.

(29) Scirè, S.; Crisafulli, C.; Minicò, S.; Condorelli, G. G.; Mauro, A. D. *J. Mol. Catal. A: Chem.* **2008**, 284, 24–32.

(30) Calla, J. T.; Davis, R. J. *J. Catal.* **2006**, 241, 407–416.

(31) Schubert, M. M.; Venugopal, A.; Kahlich, M. J.; Plzak, V.; Behm, R. J. *J. Catal.* **2004**, 222, 32–40.

(32) Daté, M.; Haruta, M. Moisture Effect on CO Oxidation over Au/TiO_2 Catalyst *J. Catal.* **2001**, 201, 221–224.

(33) Manasilp, A.; Gulari, E. *Appl. Catal. B: Environ.* **2002**, 37, 17–25.

(34) Manzoli, M.; Avgouropoulos, G.; Tabakova, T.; Papavasiliou, J.; Ioannides, T.; Boccuzzi, F. *Catal Today* **2008**, 138, 239–243.

(35) Avgouropoulos, G.; Ioannides, T.; Papadopoulou, C.; Batista, J.; Hocevar, S.; Matralis, H. K. *Catal. Today* **2002**, 75, 157–167.

(36) Luengnaruemitchai, A.; Naknam, P.; Wongkasemjit, S. *Ind. Eng. Chem. Res.* **2008**, 47, 8160–8165.